Journal of Luminescence 197 (2018) 147–152

Contents lists available at ScienceDirect

Journal of Luminescence

journal homepage: www.elsevier.com/locate/jlumin

Preparation of highly fluorescent sulfur doped graphene quantum dots for live cell imaging

Kaixiang Jin[a,1], Hui Gao[a,*,1], Luhao Lai[b], Yuqian Pang[a], Shiyuan Zheng[c], Yongyan Niu[c], Xiaolong Li[d,*]

[a] School of Physical Science and Technology, Key Laboratory for Magnetism and Magnetic Materials of Ministry of Education, National & Local Joint Engineering Laboratory for Optical Conversion Materials and Technology, Key Laboratory of Special Function Materials and Structure Design, Ministry of Education, Lanzhou University, Lanzhou 730000, PR China

[b] School of Basic Medical Sciences, Lanzhou University Key Laboratory of Preclinical Study for New Drugs of Gansu Province, Lanzhou 730000, PR China

[c] School of Life Sciences, Key Laboratory of Cell Activities and Stress Adaptations, Lanzhou University, 222 South Tianshui Rd, Lanzhou, Gansu 730000, PR China

[d] Shanghai Synchrotron Radiation Facility, Shanghai Institute of Applied Physics, Chinese Academy of Sciences, Shanghai 201204, PR China

ARTICLE INFO

Keywords:
Sulfur doping
Graphene quantum dots
Cell bio-imaging

ABSTRACT

Herein, we reported a facile one-step hydrothermal strategy to synthesize stable, strong blue fluorescence and water-soluble sulfur doped graphene quantum dots (S-GQDs) with the citric acid (CA) and powdered sulfur (S) as the precursors. The results indicated that S atoms were successfully introduced into the structure of graphene, and sulfur doping indeed improved the intensity of blue emission of GQDs. The as-prepared S-GQDs, as the effective cell-imaging material, would easily penetrated into the cell membranes of Hela cell and exhibited relatively low cytotoxicity. When treated with the typical bacteria medium (*Staphylococcus aureus LZ-01 and Escherichia coli DH5α*), it also did not show the conspicuous antiseptic qualities. Therefore, the S-GQDs would have potential applications in the bio-imaging.

1. Introduction

Graphene quantum dots (GQDs) have attracted tremendous attention due to their excellent properties including high water solubility, low cytotoxicity, excellent biocompatibility and high resistance to photobleaching [1]. They also have wide range of applications in the field of photocatalysts, bio-imaging, ions detection, and electrochemical luminescence [2–5]. Generally, there are two approaches for preparation of GQDs, including “top-down” and “bottom-up” methods. Bottom-up methods have obvious advantages in adjusting the composition and physical properties of GQDs by choosing organic precursors or changing the reaction conditions. Bottom-up methods could also provide the effective way for doping heteroatoms into the structure of GQDs. As it known, doping other atoms could change the electronic density and effectively tune optical and electrical properties of GQDs [6]. Until now, a large number of researches have focused on the synthesis and properties of nitrogen doped graphene quantum dots (N-GQDs) [7]. Compared with the N-GQDs, sulfur doped graphene quantum dots (S-GQDs) also attracted much attentions for the reported excellent abilities, such as the electrocatalytic activity [8], hydrogen adsorption [9], high electrochemical capacity [10] rechargeable battery performance [11], and p-type semiconductor property [12]. It is of scientific interest and technical importance to investigate the optical and biological properties of S-GQDs.

However, sulfur doping is commonly realized by sulfur compounds (such as thiourea), which would be toxic with unpleasant smell [6]. Herein, we reported a facile and low cost hydrothermal route to synthesize S-GQDs by directly using the inexpensive and nontoxic powdered sulfur as the S source. The as-prepared S-GQDs exhibited strong blue fluorescence as well as the good water-solubility. And for bio-imaging measurements, the S-GQDs shows the low cytotoxicity and excellent cell-imaging for Hela cells. Moreover, when incubated with the typical bacteria medium (*Staphylococcus aureus LZ-01 and Escherichia coli DH5α*), it showed the weak antiseptic qualities. Therefore, the S-GQDs would have potential applications in the bio-imaging.

* Corresponding authors.
E-mail addresses: hope@lzu.edu.cn (H. Gao), lixiaolong@sinap.ac.cn (X. Li).
[1] These authors contributed equally to this work.

https://doi.org/10.1016/j.jlumin.2018.01.028
Received 7 September 2017; Received in revised form 31 December 2017; Accepted 18 January 2018
Available online 06 February 2018

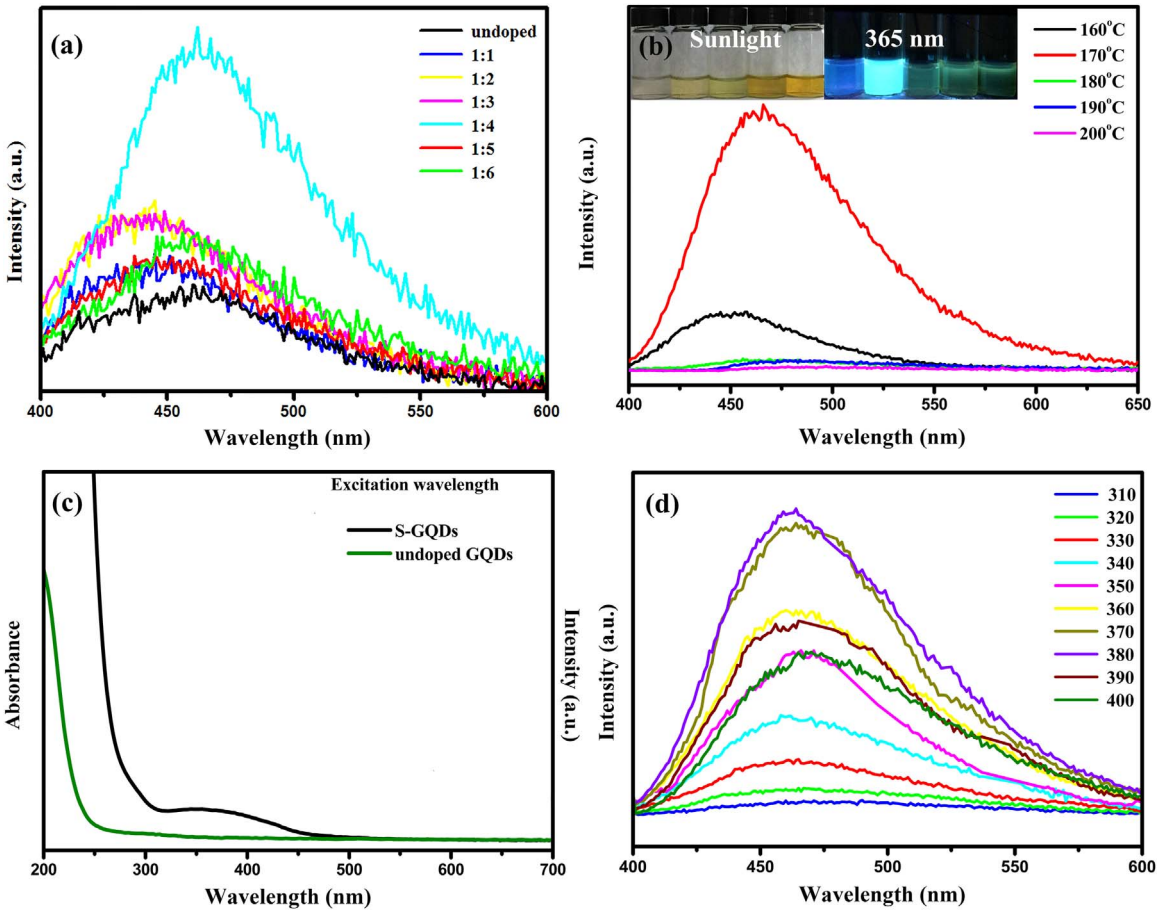

Fig. 1. (a) The emission spectra of S-GQDs under different ratios from1:1 to 1:6 (λ_{ex} = 365 nm). (b) The emission spectra of S-GQDs under synthesizing temperatures from 160 °C to 200 °C. The insets are optical images of S-GQDs aqueous solution under different temperatures and the diluted solution excited by 365 nm. (c) The absorption and the absorption of undoped GQDs. (d) The emission spectra of S-GQDs under different excitation wavelengths of 310–400 nm.

2. Experimental

2.1. Synthesis of S-doped GQDs

0.21 g (1 mmol) CA and 0.128 g (4 mmol) powdered S were dissolved into 5 ml deionized water. Then the solution was transferred into a 20 ml Teflon lined stainless autoclave. The sealed autoclave was heated to 170 °C in an electric oven and kept for additional 4 h. The final product was collected by adding ethanol into the solution and centrifuged at 5000 rpm for 5 min. The solid can be easily re-dispersed into water.

2.2. Cell imaging

Hela cells (the concentration of 2*105/hole) were plated on a 30-mm Petri dish in culture medium one day in advance for cell imaging. For in vitro study, cells were incubated in medium containing S-GQDs for 24 h, then treated with PBS for two times to wash the unabsorbed free dots. The whole system was imaged on laser scanning confocal microscopy (LSCM-710)

2.3. Methyl thiazolyl tetrazolium (MTT) assay

The cytotoxicity was assessed using the classic MTT assay with Hela cells. The liquid culture was poured to leave the adherent culture of Hela cells digested by E enzyme. When the digestion is finished, the cells were completely separated from the wall and dispersed evenly after percussed by 3 ml serum containing medium 1640. Using the counting plate, cell suspension with a suitable concentration certain volume were seeded into the 96-well plate at ~ 5 × 10^3 cells per well. The cells were incubated for 12 h in a humidified atmosphere at 37 °C under 5% CO_2. The S-GQDs solutions at various concentrations (10, 100, 200, 500 and 1000 μg/ml) were added to the wells and the cells were incubated for 72 h at the above cell culture conditions. A solution of 20 μL MTT (5 mg/ml) was then added into the wells and incubated for 4 h at 37 °C. Finally, the culture solution is dried and the dark blue formazan crystals were left at the bottom of the hole. Dimethyl sulphoxide (DMSO) was added to dissolve the formazan completely. The formazan concentrations were quantified using an enzyme-linked immunosorbent assay reader (ELISA FlexStation 3) to measure the absorbance at 570 nm. Parallel detection of 4 holes in each experiment were carried twice.

2.4. Experiment of inhibition zone

Put the beef Extract peptone agar medium which has been sterilized and cooled to about 50 °C respectively into two sterile plates, then placed the plates horizontally until the agar freeze. Use sterile straw to absorb 0.2 ml *Staphylococcus aureus LZ-01 and Escherichia coli DH5α* (from Ministry of Education Key Laboratory of Cell Activities and Stress Adaptations) bacteria suspension which have been cultivated for 18 h and add them into two sterile plates respectively, use sterile triangle coating bar to coat them evenly. Divided the even flat plate into 4 parts, marking each part with its reagent name. Use sterile tweezers to pick up the small round sterilized filter paper (D5 mm) and immersed them into the tube with aqueous solution of CA and S-GQDs in it, then soak the filter paper. (When removing the filter paper, guarantee that the amount of the solution in each paper basically consistent) With aseptic

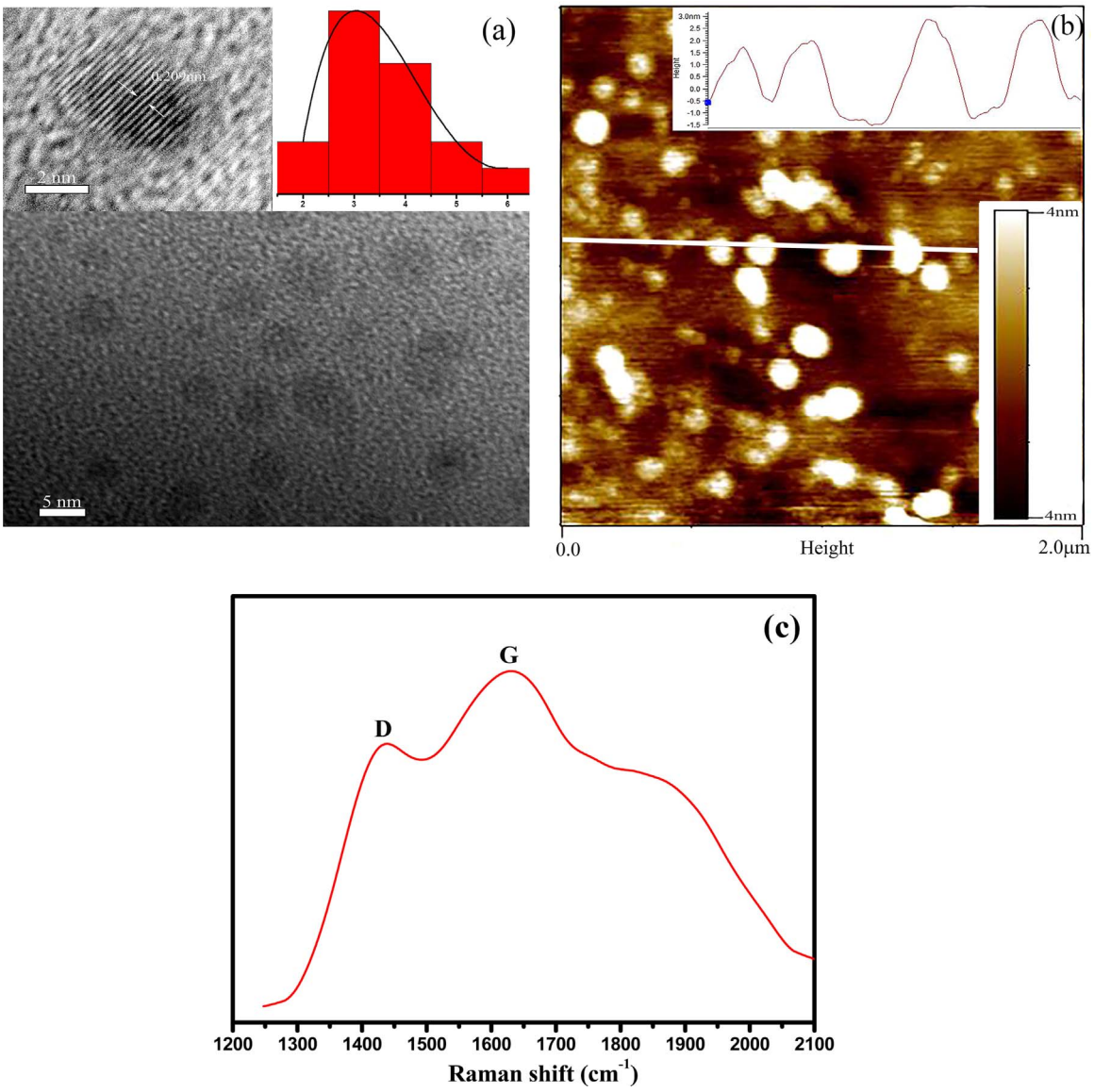

Fig. 2. (a) TEM image of S-GQDs. The corresponding size distribution and high-resolution TEM image are inserted as insets. (b) AFM image of S-GQDs. (c) The Raman spectrum of S-GQDs.

operation, paste the filter paper to the corresponding region of plate. After the paste, put the plates containing bacteria upside down in 37 °C constant temperature incubator for 24 h, then take them out and observe the size of the inhibition zone.

2.5. Characterization

The transmission electron microscopy (TEM) observation was conducted on an F-30 S-TWIN electron microscope (Tecnai G2, FEI Company). Atomic force microscope (AFM) images were recorded with MFP-3D-SA. X-ray photoelectron spectra (XPS, PHI-5702, Physical Electronics) were obtained using a monochromated Al-Ka irradiation. The ultraviolet-visible (UV–vis) absorption spectra were recorded with a PerkinElmer 950 spectrophotometer. The PL spectra and fluorescence emission spectra were recorded using an FLS-920T fluorescence spectrophotometer and a HORIBA JOBIN YVON Fluorolog-3 Spectrofluorometer system, respectively. All the experiments were conducted under Normal Temperature and Pressure.

3. Results and discussion

The fluorescent behavior of the S-GQDs is affected by the ratio between the CA and powered S as well as the temperature of the reaction. Therefore, conditions of the reaction need to be optimized in order to obtain the highest luminescent S-GQD. Fig. 1(a) showed the change of the emission intensity of S-GQDs with different S doping amounts (The excitation wavelength is 365 nm). We can clearly see that S-GQDs have the strongest luminescence when the ratio of CA: powdered S is 1:4. And the optimum temperature of hydrothermal reaction is 170 °C, as shown in Fig. 1(b). With the increasing of reaction temperature, the emission wavelengths varied from 445 to 478 nm and the maximum emission wavelength is 460 nm. The insets show the image of S-GQDs under sunlight and excited by 365 nm and the result indicates that the brightest S-GQDs is the second one, which is in accord with the optimum temperature. Although the mechanism is still not clear, there is a possibility that excessively high temperature introduced a large number of S atoms to cover the surface of S-GQDs, resulting in the decrease of the fluorescence of S-GQDs [13]. The UV–vis absorption is shown in Fig. 1(c). For the S-GQDs, there is an absorption peak at 350 nm but the undoped S-GQDs do not have an absorption peak. As the excitation

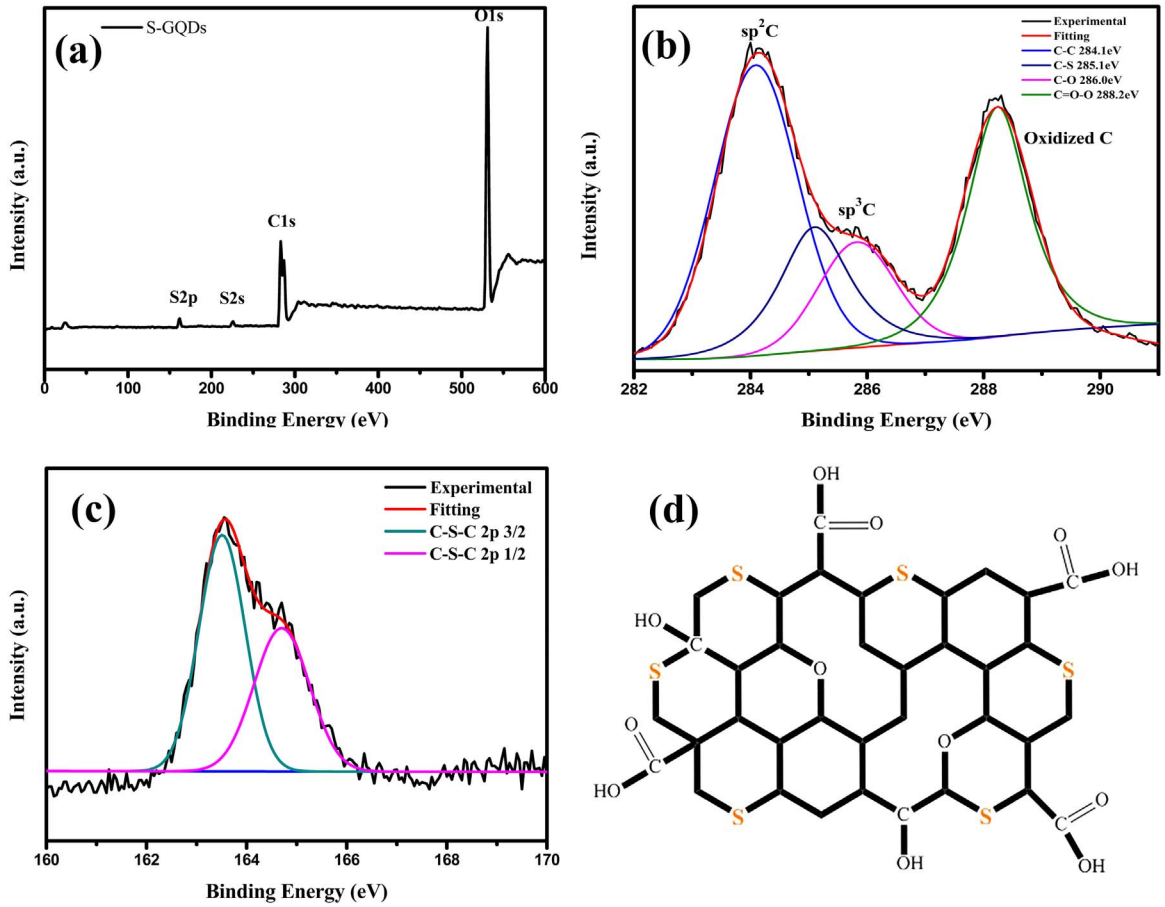

Fig. 3. (a) XPS full spectrum of S-GQDs. The high resolution XPS spectra of C1s (b) and S2p (c). (d) The image of the structure of S-GQDs.

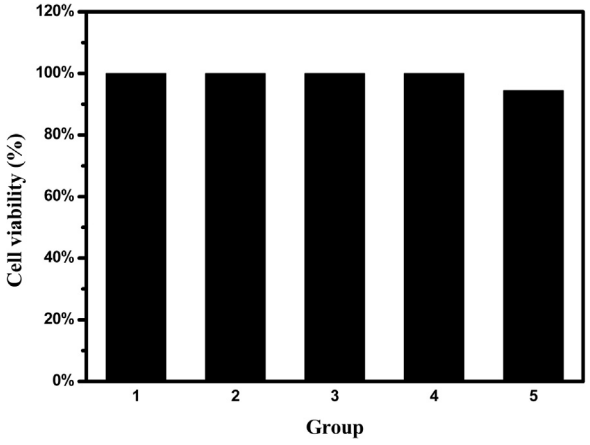

Fig. 4. The cell viabilities of different concentrations of the S-GQDs (Group 1–5: 10, 100, 200, 500 and 1000 μg/ml).

wavelength gradually increased from 310 nm to 400 nm, the emission of S-GQDs was located at 460 nm, which are independent of excitation wavelengths, and the maximum intensity of emission was obtained with an excitation wavelength of 380 nm. The fluorescent intensity of S-GQDs is about 22 times stronger than that of undoped GQDs. Consisting with the former report, doping sulfur could introduce the surface states with a concomitant effect for enhancing the fluorescence of S-GQDs [13].

TEM (Fig. 2(a)) showed the size of S-GQDs ranging from 1.85 nm to 6.04 nm and the average diameter is about 3.93 nm. High resolution TEM (HRTEM) clearly displayed the discernible in-plane graphite lattice structure with the lattice spacing of 0.209 nm. According to the AFM image (Fig. 2(b)), the S-GQDs are uniform in size and well dispersed. The average height of S-GQDs is 3.0 nm. Raman spectrum (Fig. 2(c)) showed the disordered (D) band at 1432 cm^{-1} and the graphite (G) band at 1630 cm^{-1}, respectively. The ratio of intensities (I_D/I_G) of these bands is 0.78, which indicates that the S-GQDs are crystalline and graphitic.

X-ray photoelectron spectroscopy was used to measure the composition of the S-GQDs. The full scan XPS spectrum of S-GQDs, as shown in Fig. 3(a), presents 4 peaks at ~ 164 eV, ~ 227 eV, ~ 284 eV and ~ 533 eV correspond to S2p, S1s, C1s and O1s, respectively and the S-GQDs contain O 73.76%, C 22.40% and S 3.85%. It suggested that S is successfully doped into the GQDs. According to the previous reports, nitrogen (N) can easily enter the GQDs, owing to the C and the N have similar chemical and physical properties [1]. But S atoms have a larger diameter than that of C atoms, therefore, only small sulfur could be doped into the structure of graphene. The high resolution spectra of the C1s can be fitted into 4 Gaussian peaks (Fig. 3(b)) at 284.1, 285.1, 286.0 and 288.2 eV, which attribute to sp^2 C (C-C), sp^3 C (C-S and C-O) and Oxidized C (C=O-O), respectively and the percentages are 47.9%, 19.6% and 32.4%, respectively. The high resolution of the S 2p XPS spectrum of S (Fig. 3(c)) clearly shows 2 peaks at 163.5 and 164.7 eV, which are assigned to S 2p3/2 and S 2p1/2. According to the XPS results and previous report [7], as shown in Fig. 3(d), the CA forms graphene framework through intermolecular dehydrolysis and S atoms enter the GQDs to form C–S bonds.

The strong fluorescent characteristic of the S-GQDs make it possible to explore their application in biological imaging. Firstly, it is essential to probe the cytotoxicity of S-GQDs by using the MTT assay. Fig. 4 depicted the cell viability studies under various concentrations of the S-

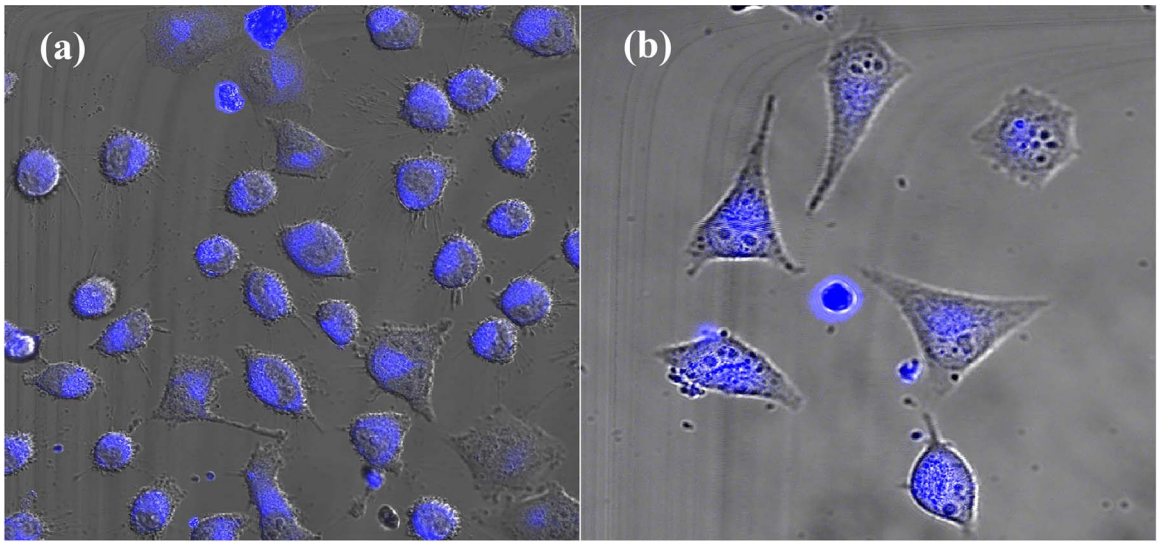

Fig. 5. (a) Fluorescent images of hela cell after incubation with S-GQDs for 24 h. (b) Partial enlarged drawing of fluorescent images of hela cell after incubation with S-GQDs for 24 h.

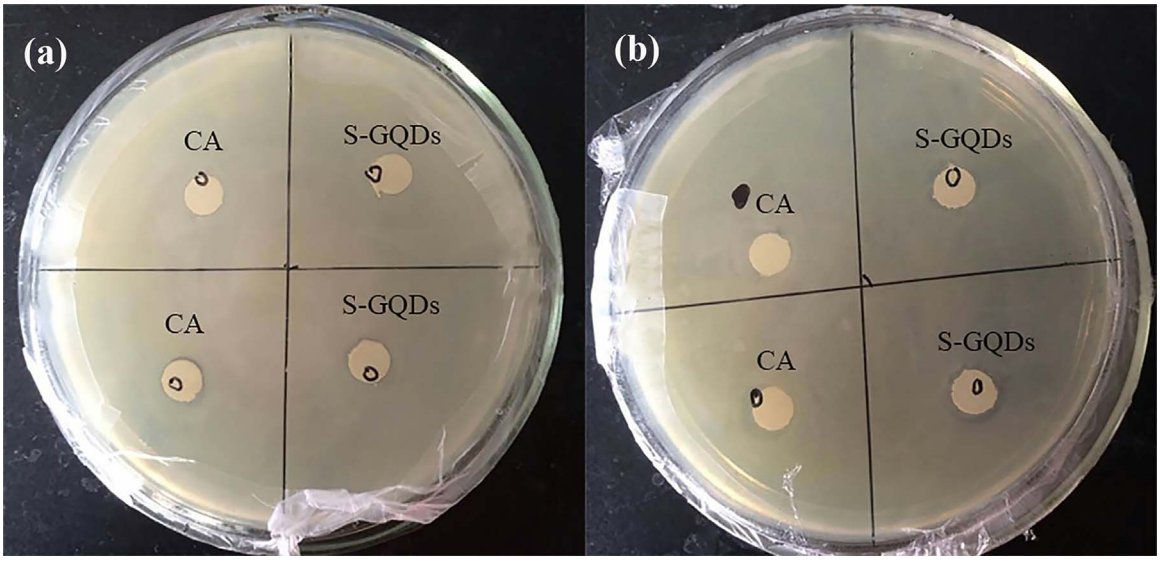

Fig. 6. *Staphylococcus aureus LZ-01* medium (a) and *Escherichia coli DH5α* medium (b) with CA as well as S-GQDs.

GQDs (Group 1–5: 10, 100, 200, 500 and 1000 μg/ml). When the concentration of S-GQDs approached to the 1000 μg/ml, the cell viability has a slight descent. This result demonstrated that the S-GQDs indeed have a low cytotoxicity. After incubating Hela cells with the S-GQDs for 4–24 h, the live cells were imaged with a laser scanning confocal microscope under 365 nm laser excitation. No morphological change of the cells was observed after incubation with S-GQDs, further confirming their low cytotoxicity to living cells. These S-GQDs, as shown in Fig. 5(a), (b), could easily penetrate into the cell membranes to reach the cytoplasm but not to the nuclei, which is in accord with previous studies that the interaction of living cells with nanomaterials would not lead to genetic disruption and toxicity to the cells [14].

To our knowledge, the bacteria are more vulnerable to damage than the cells, because the bacteria bear a nucleus without nuclear membrane, which are different from the cells. Therefore, it is also important for us to investigate the influence of S-GQDs when incubating with bacteria. Determining the potency of antibiotics were investigated and assessed through measuring minimum inhibitory concentration (MIC), diameter of zone of inhibition [15]. Herein, we choose *Staphylococcus aureus LZ-01 and Escherichia coli DH5α* as the typical indicator bacteria. In order to guarantee the accuracy of experiment, the CA solution was chosen as the control group. As shown in Fig. 6(a) and (b), the control group had no clear zone of inhibition, which indicated that the solvent had no influence on the bacteria. As shown in the Fig. 6(a) and (b), the diameter of zone of inhibition is very small and inhibitory zone is foggy. It suggested that S-GQDs would have weak antiseptic qualities. These results indicated that S-GQDs have an excellent biocompatibility both for the cell and bacteria.

4. Conclusions

We chose the inexpensive and nontoxic powdered sulfur as the S source to synthesize highly luminescent S-GQDs by a facile one-step hydrothermal method. The effective doping of sulfur improve the fluorescent intensity of S-GQDs. The as-prepared S-GQDs would easily penetrated into the cell membranes of Hela cell and exhibited relatively low cytotoxicity. Also, when S-GQDs was incubated with the typical bacteria medium (*Staphylococcus aureus LZ-01 and Escherichia coli DH5α*), it shows weak antiseptic qualities. The study indicates that sulfur doping can effectively improve the optical properties of GQDs, showing great potential applications in bio-imaging.

Acknowledgements

This work was financially supported by the National Natural Science Foundation of China (Grant nos. 51402140 and U1632129) and the Fundamental Research Funds for the Central Universities (lzujbky-2016-128).

References

[1] B.-X. Zhang, H. Gao, X.-L. Li, Synthesis and optical properties of nitrogen and sulfur co-doped graphene quantum dots, New J. Chem. 38 (2014) 4615.
[2] S.N. Baker, G.A. Baker, Luminescent carbon nanodots: emergent nanolights, Angew. Chem. 49 (2010) 6726–6744.
[3] H. Li, Z. Kang, Y. Liu, S.-T. Lee, Carbon nanodots: synthesis, properties and applications, J. Mater. Chem. 22 (2012) 24230.
[4] L. Li, G. Wu, G. Yang, J. Peng, J. Zhao, J.-J. Zhu, Focusing on luminescent graphene quantum dots: current status and future perspectives, Nanoscale 5 (2013) 4015.
[5] L. Cao, M.J. Meziani, S. Sahu, Y.-P. Sun, Photoluminescence properties of graphene versus other carbon nanomaterials, Acc. Chem. Res. 46 (2012) 171–180.
[6] D. Qu, M. Zheng, P. Du, Y. Zhou, L. Zhang, D. Li, H. Tan, Z. Zhao, Z. Xie, Z. Sun, Highly luminescent S, N co-doped graphene quantum dots with broad visible absorption bands for visible light photocatalysts, Nanoscale 5 (2013) 12272–12277.
[7] D. Qu, M. Zheng, L. Zhang, H. Zhao, Z. Xie, X. Jing, R.E. Haddad, H. Fan, Z. Sun, Formation mechanism and optimization of highly luminescent N-doped graphene quantum dots, Sci. Rep. 4 (2014) 5294.
[8] Z. Yang, Z. Yao, G. Li, G. Fang, H. Nie, Z. Liu, X. Zhou, X. Chen, S. Huang, Sulfur-doped graphene as an efficient metal-free cathode catalyst for oxygen reduction, ACS Nano 6 (2012) 205–211.
[9] Y. Xia, Y. Zhu, Y. Tang, Preparation of sulfur-doped microporous carbons for the storage of hydrogen and carbon dioxide, Carbon 50 (2012) 5543–5553.
[10] M. Seredych, K. Singh, T.J. Bandosz, Insight into the capacitive performance of sulfur-doped nanoporous carbons modified by addition of graphene phase, Electroanalysis 26 (2014) 109–120.
[11] Y. Li, J. Wang, X. Li, D. Geng, M.N. Banis, Y. Tang, D. Wang, R. Li, T.-K. Sham, X. Sun, Discharge product morphology and increased charge performance of lithium–oxygen batteries with graphene nanosheet electrodes: the effect of sulphur doping, J. Mater. Chem. 22 (2012) 20170.
[12] H. Gao, Z. Liu, L. Song, W. Guo, W. Gao, L. Ci, A. Rao, W. Quan, R. Vajtai, P.M. Ajayan, Synthesis of S-doped graphene by liquid precursor, Nanotechnology 23 (2012) 275605.
[13] X. Li, S.P. Lau, L. Tang, R. Ji, P. Yang, Sulphur doping: a facile approach to tune the electronic structure and optical properties of graphene quantum dots, Nanoscale 6 (2014) 5323–5328.
[14] J. Jeong, M. Cho, Y.T. Lim, N.W. Song, B.H. Chung, Synthesis and characterization of a photoluminescent nanoparticle based on fullerene-silica hybridization, Angew. Chem. 48 (2009) 5296–5299.
[15] H. Men, J. Zhang, C. Wang, Measurement of Inhibition Zone Based on Cellular Automata Edge Detection Method, 2009, pp. 357–360.